ISSN 2411-3336; e-ISSN 2541-9404

JOURNAL OF MINING INSTITUTE

Zapiski Gornogo instituta

Journal homepage: pmi.spmi.ru

Research article

Geology

Insights into field surveying and automated processing of digital outcrop models for fracture analysis

Oksana V. Lunina✉, Aleksei S. Nizovtsev,

Institute of the Earth's Crust SB RAS, Irkutsk, Russia

How to cite this article: Lunina O.V., Nizovtsev A.S. Insights into field surveying and automated processing of digital outcrop models for fracture analysis. Journal of Mining Institute. 2026. Vol. 280, p. 163-175.

Abstract

When automatically extracting fracture attitudes from a dense point cloud, there are challenges that complicate the correct characterization of the outcrop disrupted by certain fracture sets. In this regard, experimental and methodological studies were carried out to analyze fractures and their associated sets, which were extracted using an automated method to identify satisfactory conditions for data collection and processing. Primary data were acquired using a DJI Phantom 4 RTK unmanned aerial vehicle in the Primorsky and North Baikal deep fault zones of the Baikal rift. Structure from Motion photogrammetry was used to create dense point clouds. The obtained results show that the unidirectional camera orientation and the exposure of a single wall of the rock outcrop present a challenge for determining fracture sets. However, selecting a fragment of the digital outcrop model (DOM) facing various cardinal directions helps avoid orientation bias in the stereographic projections of poles to fractures and provides high-precision data on the fracture pattern. A well-chosen fragment of the DOM accurately represents fracture sets of the overall outcrop, saving time and computational resources. When the structural environment changes, the DOM allows for an analysis of the fracture pattern at any outcrop section, thereby improving the quality and productivity of the work. In the case of limited processing power, it is sufficient to use a dense point cloud of medium quality to extract fractures and their sets. The correct automated identification of fracture sets enhances the efficiency of rock deformation analysis in the field of engineering geology and mineral resource development.

Keywords

fractures; dip and strike; sets; digital outcrop model; unmanned aerial photography; software

Funding

This study was funded by Russian Science Foundation grant 25-27-00565, https://rscf.ru/project/25-27-00565/.

Received: 27.02.2026 ***Accepted: 25.06.2026*** ***Online: 10.09.2026*** ***Published: 10.09.2026***

Introduction

Fracture analysis is used to examine rock deformations and the degree of their disruption. It is also applied to mapping fault lines and their associated zones, as well as to studying the kinematic processes of material movement and the dynamic conditions that controlled structure formation (i.e., the direction and nature of the stresses that caused the deformation; a specific aspect is known as tectonophysical analysis). Traditionally, almost all studies of the fracture networks in outcrops are based on measuring the fracture attitude using a geological compass and counting their number per unit length, area, or volume with a manual approach [1]. Mobile phones with specialized applications (e.g., GeoCompass) are used less frequently. Routine fracture surveys are often conducted across a limited area of 10-20 m, regardless of the size of the outcrop. The heterogeneity of the outcrop structure is documented qualitatively in descriptions, sketches, and photography.

This is an open access article under the CC BY 4.0 license

In recent years, advances in unmanned aerial vehicle (UAV) technology and specialized software for building and processing digital outcrop models (DOM) have opened up unique opportunities to acquire and analyze significantly more data on rock mass fracturing. Dense point clouds and photorealistic textured 3D models of the rock masses are created using remote sensing methods implemented in software such as Agisoft Metashape (formerly Agisoft PhotoScan) [2-4], ShapeMetriX [5, 6], 3DM Analyst [7], Sirovision, and others. Subsequently, mathematical algorithms are applied to DOM to identify fractures and their principal sets [8], including through the use of computer programs such as Discontinuity Set Extractor (DSE) [9-11] and CloudCompare with plugins [12-14], as well as machine learning techniques [15]. Using the output data from DSE and CloudCompare, it is possible to calculate the spacing between fractures within each set [16], the stability parameters of the rock mass [17], and the fracture density over the entire outcrop surface, quantified using various parameters in the DICE module for MATLAB [18]. Virtual reality applications have also been proposed for DOM of rock masses [19].

The earliest studies on fracture analysis in a digital environment focused on comparing the results derived from photogrammetric processing of aerial imagery, lidar surveys, and traditional compass measurements [20, 21]. Later research developed approaches for extracting attitude data not only for fractures but also for dikes, slickensides, and other structures [22], as well as for calculating fracture intensity [13, 23]. Digital models can be applied repeatedly to solve various geological-structural and geomechanical problems, and is positioned as a modern method for studying the geological environment [24], particularly in hard-to-reach areas [25], where safety and time constraints are critical [26]. The articles [27, 28] present comprehensive reviews on DOM application and the automated extraction of fracture characteristics from dense point clouds.

Despite the advantages of digital technologies for fracture analysis, most published DOM-based studies rely on a semi-automatic method to extract fracture attitude data, whereby fractures are either digitized or manually picked by clicking on the discontinuity surface in the image. The automated approach often yields only one or, occasionally, two, fracture maxima on stereographic projections of normal vector poles [29-31], which is insufficient for tectonophysical analysis aimed at stress reconstruction using paragenetic methods [32, 33]. In reality, the fracturing of any rock mass is characterized by at least three main fracture sets, which differ in azimuths and/or dip angles.

Other problems associated with digital outcrop analysis are time consumption and compute resources. Even on sufficiently powerful workstations, constructing and processing DOM can exceed 24 h. Thus, an optimal approach is required for remote data acquisition and subsequent automated analysis of fracture networks in outcrops. The aim of this study is to conduct methodological experiments on the analysis of fractures and their sets, extracted automatically in well-known software packages to find satisfactory conditions for data acquisition and processing that will facilitate the use of digital outcrop models for fracture analysis and their more meaningful integration into the practice of mining and geological works.

Methods

The experimental and methodological work was carried out on five rock outcrops located within the zones of the Primorsky and North Baikal deep faults of the Baikal rift system (Fig.1). Aerial photography was done manually using a DJI Phantom 4 RTK UAV, which has a camera with a 1-inch 20 MP CMOS sensor and a mechanical shutter to avoid image distortion. An advanced sensor, the optimized wide-angle lens with a diaphragm of f/2.8-f/11 along with the processing technology make it possible to obtain detailed photos with realistic colors. The survey was carried out from a distance of 1.5 m for the Krasnoyarovskoye outcrop to the first tens of meters for the Sukhoye outcrop.

This is an open access article under the CC BY 4.0 license

The predominant camera tilt angle of 0° relative to the horizontal was gradually varied up to 45° and occasionally up to 90° (when necessary). The flight path was conducted from bottom to top, right to left, right to bottom, and so on, with drone rotations in both directions at appropriate angles determined by the outcrop morphology. The overlap between images was 75-80 %.

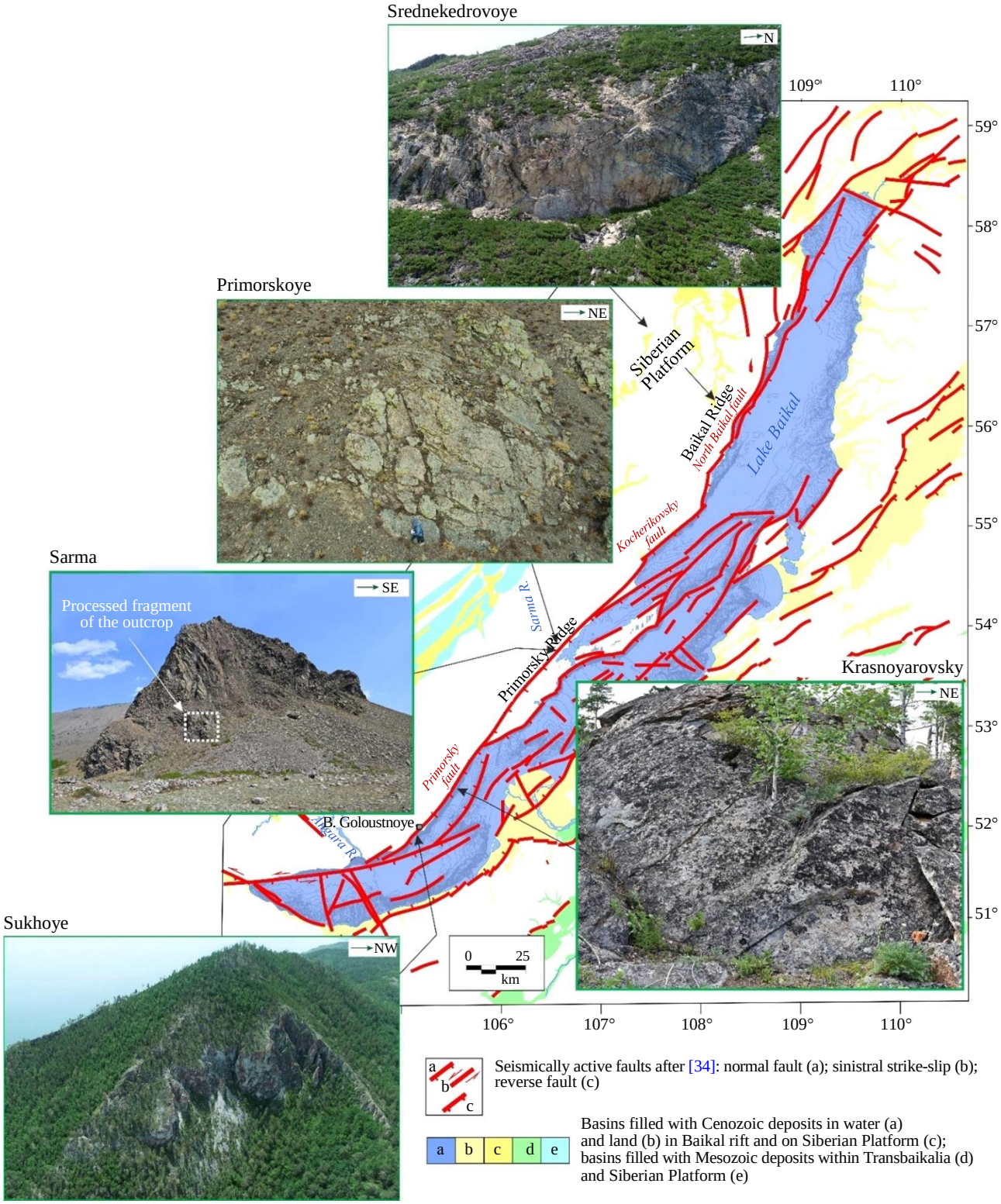


Fig.1. Location of investigated outcrops within the Baikal rift

This is an open access article under the CC BY 4.0 license

Dense point clouds, representing a type of DOM, were generated using the photogrammetric method implemented in Agisoft Metashape. Prior to processing, all defective and out-of-focus images were discarded. The following steps were then carried out automatically: image loading, image alignment, alignment optimization, and reconstruction of dense point cloud, which is similar to those from LIDAR surveys. The points in the resulting dense cloud are colored according to the spectral RGB data of the corresponding images, have spatial coordinates, and accurately describe the topography of the rock outcrop. At medium processing quality, the average point density ranged from 7115 points/m^2 at the Srednekedrovoye outcrop to 65,263 points/m^2 at the Sarma outcrop, while the Sukhoye exposure yielded 449 points/m^2. The dense point cloud, due to its discrete nature, is used for automatic extraction of fracture orientations and their sets. In contrast, the textured DOM is preferred for object visualization and geological interpretation through manual digitization of bedding planes, fractures, and other structural features.

Two well-known open-source software tools – DSE [9] and the FACETS plugin for CloudCompare [12] – were tested for extracting dip azimuths and dip angles. The construction of fracture diagrams and the identification of the main fracture sets were conducted using DSE and Dips v. 7.0 software. The latter made it possible to compare stereographic projections constructed uniformly from fracture datasets obtained by different methods. Before processing, all areas with interferences, such as vegetation, talus, and other obstructions, were removed from the dense point cloud.

In the DSE software, a fracture is defined as a set of points arranged in a plane in 3D space based on certain fitting parameters. Each point from the cloud that is classified to a plane is considered as a fracture with associated dip azimuth and dip angle, which are then used to plot the stereographic projections of poles to fractures. In CloudCompare, these points have already been combined into planes (FACETS).

Geological-structural documentation and statistical compass measurements, each comprising 100 to 103 fractures, were performed at four of the five rock exposures. The measurements were carried out following standard structural geology procedures by systematically measuring all fractures within a randomly selected ~10 m^2 section of the bedrock outcrop. For each fracture, dip azimuth and dip angle were recorded, along with, where identifiable, its genetic type (shear or extension fracture), slip surface condition, and other relevant features. Traditional description was not undertaken for the collapse bedrock scarp, exposed at a relative height of more than 300 m above Sukhoye Lake in the Semyonovka valley, 4.13 km west-southwest of the southern outskirts of the village of Bolshoye Goloustnoye (Fig.1).

Results and discussion

First test digital outcrop models of rock exposures. The results of DOM processing of the first three outcrops – the Srednekedrovoye, Primorskoye and Krasnoyarovskoye – composed of granites, showed strong agreement in the location of the main maximum on the stereographic projections of poles to fractures obtained by automated extraction and manual compass measurements (Fig.2). A major limitation, as in many earlier studies, was the apparent unipolarity of the fracture sets, which is attributed to the orientation of the main outcrop wall facing the camera. The field data also revealed systematic fracturing but the presence of only one maximum is geologically unacceptable. Thus, the authors faced the problem of the influence of the camera angle, highlighting that a certain approach to outcrop surveying and fracture pattern analysis using automated extraction is required for most geological-structural tasks (identification of main fracture sets and conjugate fracture maxima for subsequent stress field reconstruction).

A UAV survey of the fourth outcrop in the Semyonovka valley was performed on July 10, 2021, to test the feasibility of acquiring data on inaccessible rock exposures situated at high elevation and considerable distance from the researcher. According to [35], the rockfall was triggered by an earthquake 3810±100 years ago, when the collapse of a highly fractured rock mass occurred at an absolute elevation of 850 m on the right side of the valley downstream. The resulting debris blocked the drainage, forming Sukhoye Lake, which fills only intermittently in response to groundwater fluctuations (Fig.3, *a*). The headscarp, situated about 630 m on the straight from the lake floor and the operator

This is an open access article under the CC BY 4.0 license

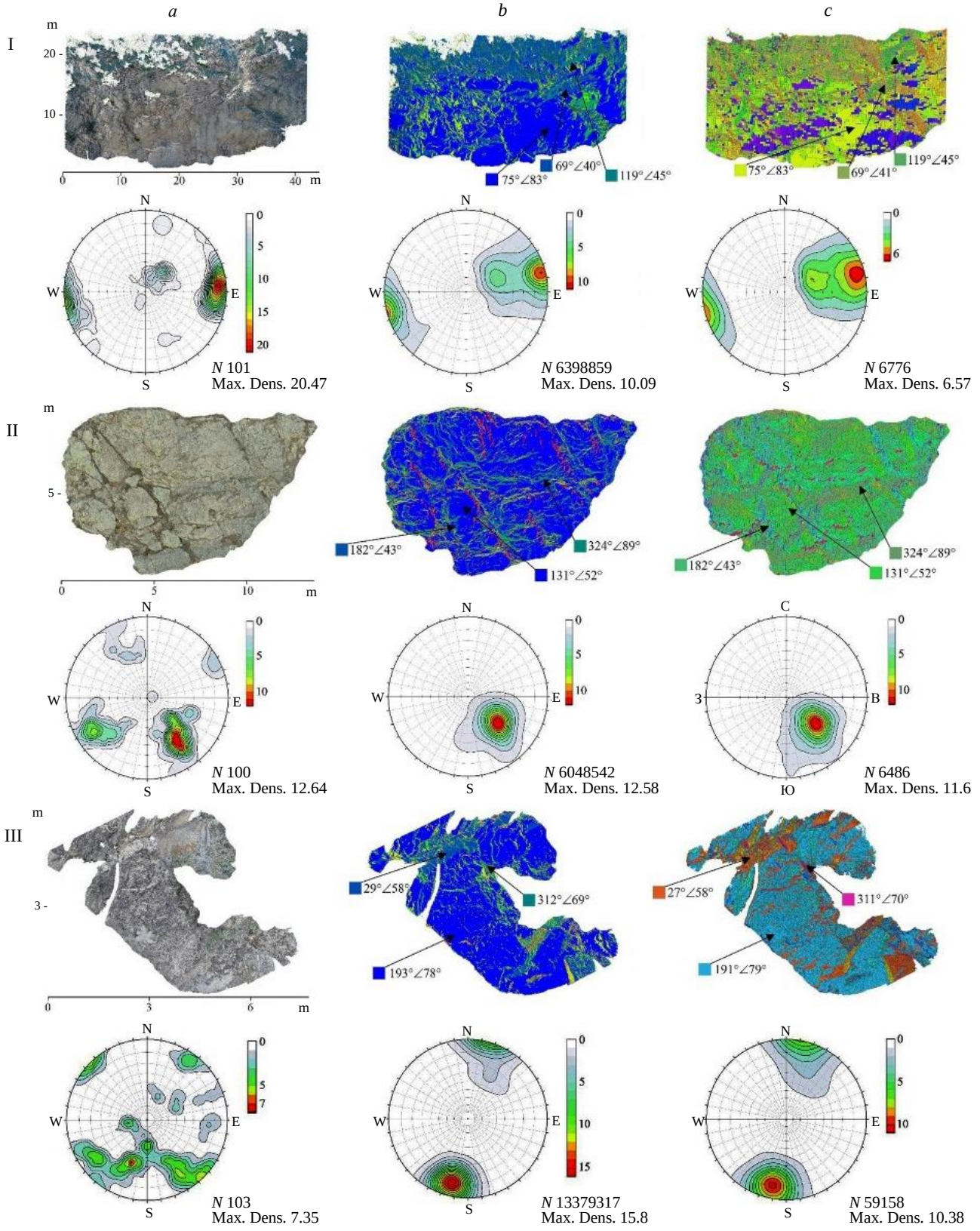


Fig.2. Results of DOM processing for the Srednekedrovoye (I), Primorskoye (II), and Krasnoyarovskoye (III) granite outcrops:
a – dense point clouds and stereographic projections of poles to fractures measured by geological compass;
b – dense point clouds classified using DSE, and stereographic projections of poles to fractures extracted using the same software;
c – dense point clouds classified using CloudCompare, and stereographic projections of poles to fractures extracted using the same software. Contours are shown at 1 % intervals. Colors in the classified dense point clouds represent individual fracture sets, with selected sets labeled; the stereoplots are presented as upper-hemisphere projections
N – number of measurements; Max. Dens. – maximum density

This is an open access article under the CC BY 4.0 license

Journal of Mining Institute. *2026. Vol. 280. P. 163-175*
© Oksana V. Lunina, Aleksei S. Nizovtsev, 2026

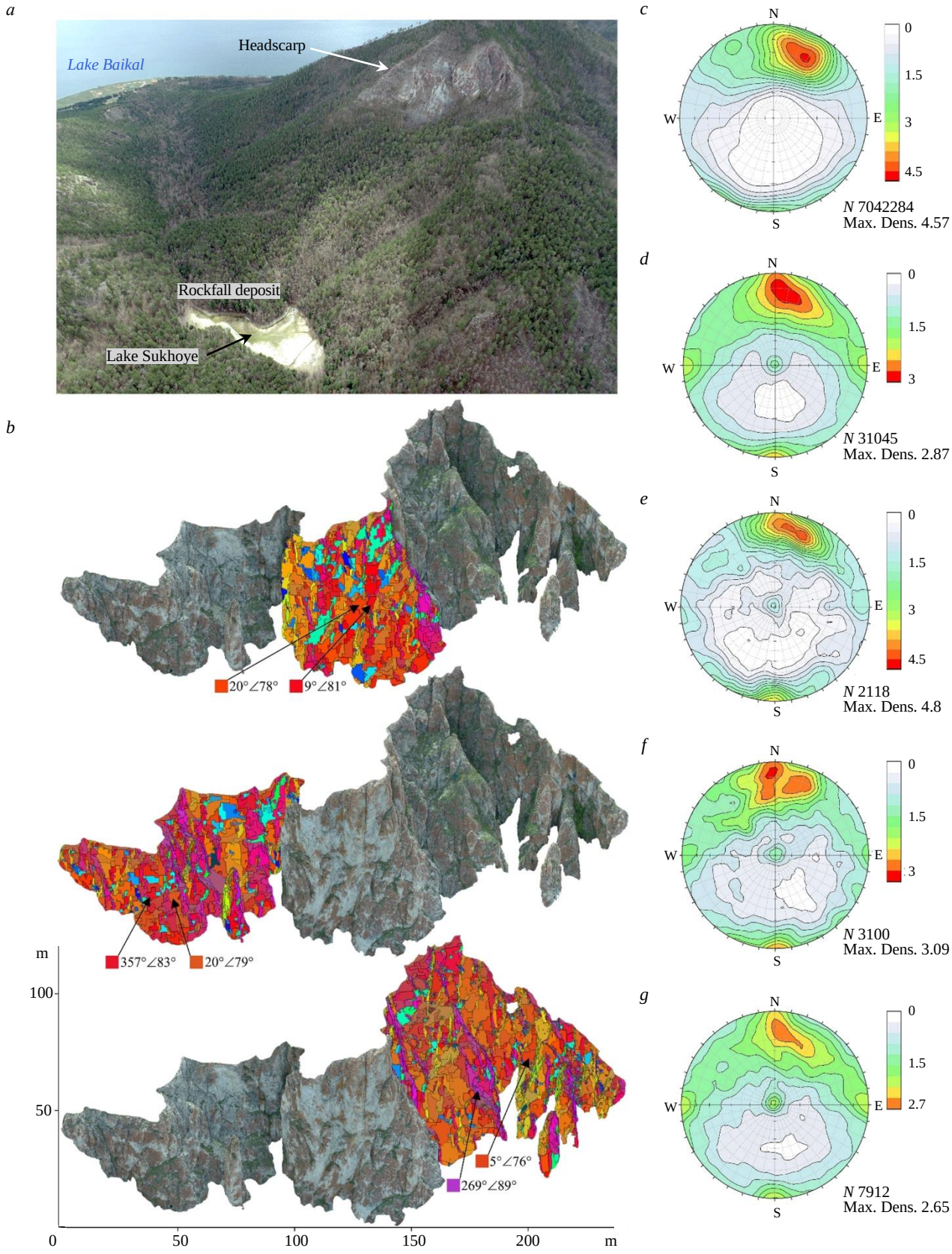


Fig.3. Results of DOM processing for the Sukhoye outcrop: *a* – the location of the rockfall headscarp formed by dolomite bedrock; *b* – the dense point cloud of the outcrop prepared for processing, with its fragments superimposed and classified in CloudCompare based on the spatial orientation of fractures; *c*, *d* – stereographic projections of poles to fractures extracted from the entire outcrop using DSE (*c*) and CloudCompare (*d*); *e-g* – stereographic projections of poles to fractures extracted from the outcrop fragments using CloudCompare. Contours are shown at 0.3 % intervals

This is an open access article under the CC BY 4.0 license

of the aerial survey, is an arcuate feature with irregular edges and a total length of 543 m. Stereographic projections of poles to fractures derived from the entire rock outcrop using DSE and CloudCompare show the dominant dip azimuths, with their maxima exhibiting a belt-like arrangement corresponding to this arc (Fig.3, *c*, *d*). Input of a large number of fractures from DSE (7,042,284 normal projections) and from CloudCompare (31,045 fractures – facets) produces only two maxima on the diagrams due to the significant dominance of fractures with certain dip azimuths and dip angles facing the camera. The principal maximum steeply dips to north-northeast (27°∠72° from DSE and 10°∠75° from CloudCompare). Splitting the outcrop into three segments reduces the dominance of camera-facing surfaces in each subset, thereby increasing the number of distinguishable maxima (Fig.3, *e*-*g*). The role of the transverse fracture sets with a nearly N-S strike is highlighted more clearly. At the same time, similarity is observed between the stereoplots constructed for the left, central, and right parts of the outcrop, as well as the invariance of the position of the main fracture sets within 10°, based on the data processed in CloudCompare.

In contrast to CloudCompare, DSE constructs normal vector poles stereographic projection as density contours and calculates the main fracture sets [21]. The number of maxima to be identified and the allowable angle between them are set as input parameters for the computation and visualization. Thus, even when one fracture set strongly dominates, DSE can still calculate several maxima, some of which – or even most – will not be expressed as contour lines but will be indicated only by a point, because their density (intensity) on the diagram is too low. It follows that for structural tasks, when only a single outcrop wall is exposed without significant protrusions, it is preferable to use either DSE or the manual mode of fracture picking in CloudCompare with the built-in Compass tool for constructing stereographic projections of poles to fractures.

Experimental and methodological studies at the Sarma outcrop. The clear effect of camera angle and azimuth on the results of automated structural analysis necessitated a targeted study of the fifth bedrock exposure of granites and granite-gneisses, located on the left bank of the Sarma River valley (see Fig.1). Classical geological-structural documentation of the outcrop with systematic fracture measurements was carried out simultaneously with aerial photography on May 26, 2022.

Accessible from three main sides, the bedrock exposure in the Sarma Gorge (Fig.4, *a*) represents an ideal object for experimental and methodological work on the investigation of fractures and their sets, identified by an automated approach. A digital twin was constructed for the entire outcrop (Fig.4, *b*), but only a prominent protrusion, which was photographed from multiple directions, was selected for the analysis (Fig.4, *c*), and proved sufficient for obtaining reliable results. Dense point clouds of this subset were classified in DSE and CloudCompare (Fig.4, *d*, *e*). Fracture stereoplots generated from field compass measurements (Fig.4, *f*), from DSE (Fig.4, *g*), and from Dips using DSE-derived data (Fig.4, *h*) demonstrate strong mutual agreement and the absence of unipolar maxima. In contrast, the maxima derived from the FACETS plugin (Fig.4, *i*) show a poorer correlation with the fracture sets revealed from field data. The main fracture set of the Primorsky fault (Fig.4, *a*) with a dip azimuth of 161°∠64° in Fig.4, *f*, 159°∠61° in Fig.4, *g*, and 159°∠59° in Fig.4, *h*, did not appear in Fig.4, *i*. Considering the algorithm underlying the FACETS program, it is reasonable to infer that the imaging process captured a considerable number of minor fractures whose dip direction faces the camera (i.e., to the southwest). If the fracture surfaces were larger, this effect would not have occurred. This finding supports the conclusion that the DSE is better suited for structural analysis in large-scale data contexts, since its point-based methodology accounts for both the number of measurements and the fracture surface area. The work on the digital twin of the Sarma outcrop demonstrates that combining a multi-directional camera angle with the selection of exposure fragments oriented toward various azimuthal directions, while considering the size of fracture surfaces, helps avoid unipolarity in the stereographic projection of poles to fractures.

This is an open access article under the CC BY 4.0 license

Journal of Mining Institute. *2026. Vol. 280. P. 163-175*
© Oksana V. Lunina, Aleksei S. Nizovtsev, 2026

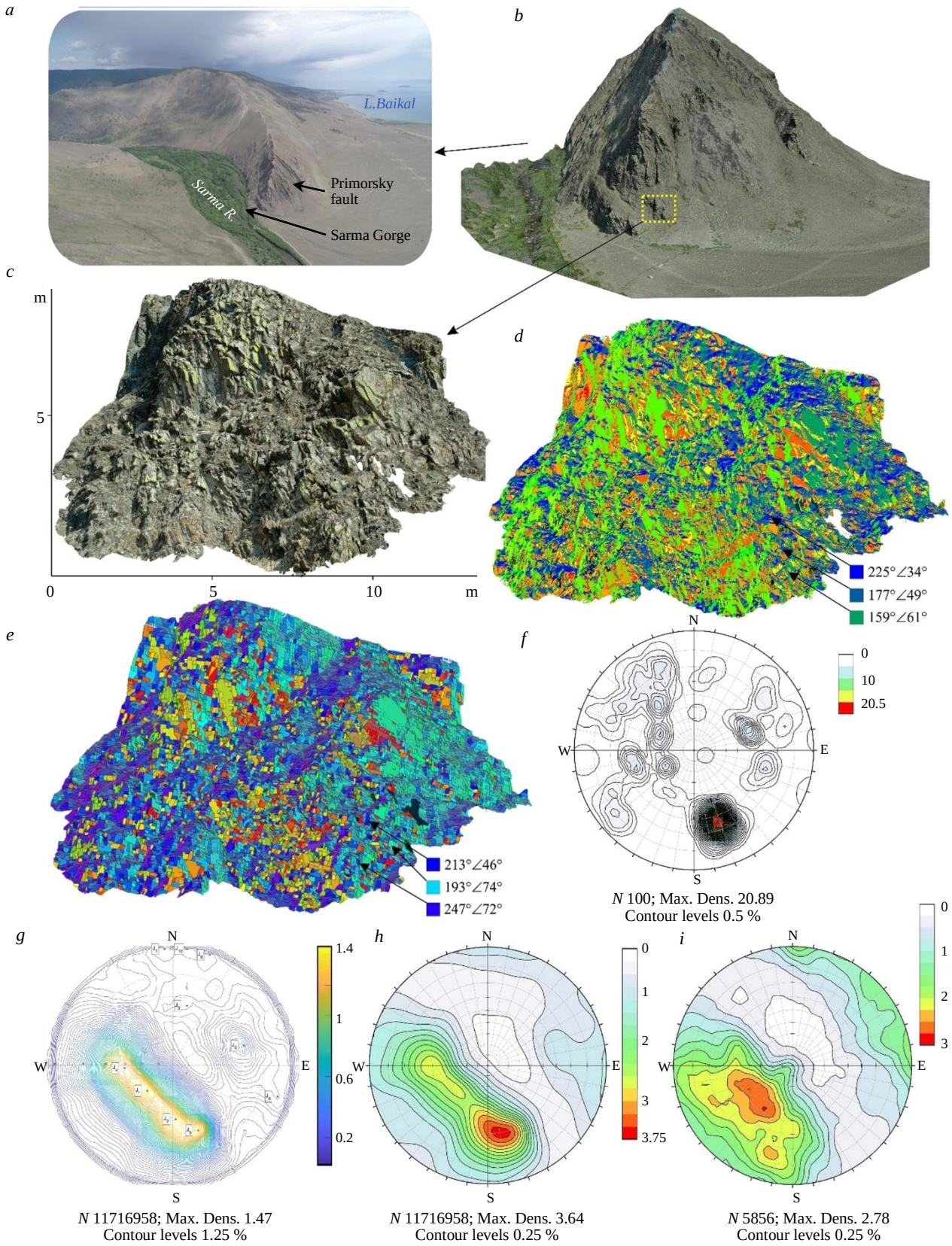


Fig.4. Results of DOM processing for the Sarma outcrop: *a* – the location of the outcrop in the Primorsky fault zone; *b* – digital model; *c* – DOM fragment; *d*, *e* – the dense point clouds classified in DSE (*d*) and CloudCompare (*e*) based on the spatial orientation of fractures; *f-j* – stereographic projections of poles to fractures measured by geological compass (*f*), extracted using DSE and plotted within it (*g*), as well as in Dips software (*h*); extracted using CloudCompare (*i*)

This is an open access article under the CC BY 4.0 license

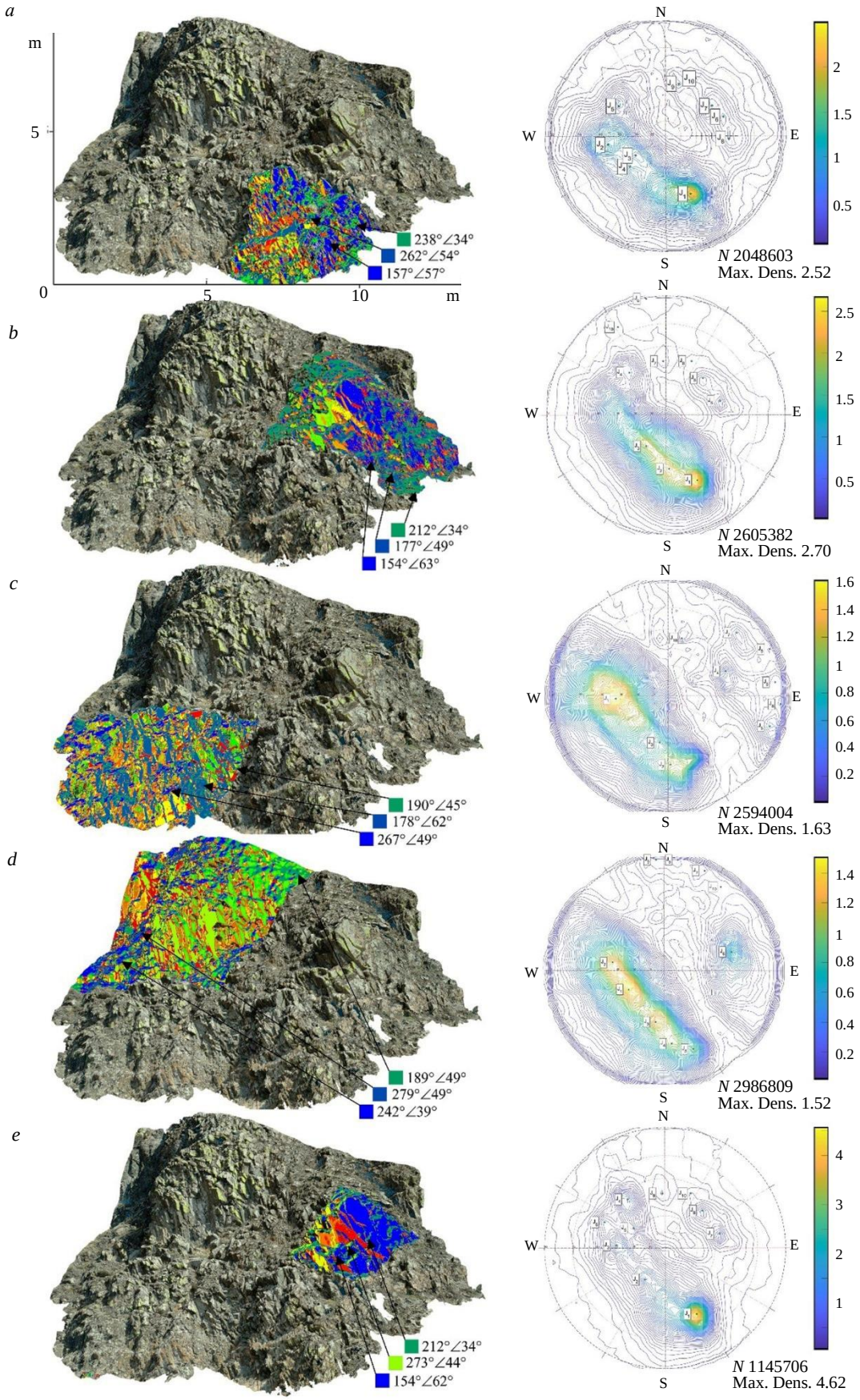


Fig.5. The dense point clouds of the Sarma outcrop classified based on the spatial orientation of fractures and corresponding stereographic projections of poles to fractures with contours shown at 1.25 % intervals: *a-d* – four parts of the tested outcrop fragments; *e* – part of the fragment shown in Fig.5, *b*. Data processing and visualization were carried out using DSE

This is an open access article under the CC BY 4.0 license

At the next stage, the tested bedrock fragment in the Sarma Gorge was subdivided into four parts, each yielding a fracture stereoplot (Fig.5, *a-d*). A smaller subarea was then extracted from the fragment in Fig.5, *b*, and fracture attitudes were analyzed (Fig.5, *e*). Testing of these and other smaller datasets showed that the main fracture maxima persist irrespective of the sampled area, although their density may vary slightly. The principal fracture sets match those on the composite stereoplot for the entire outcrop, whether derived from field measurements (see Fig.4, *f*) or DSE processing (see Fig.4, *g*). Thus, stereographic projections of poles to fractures from a fragment are representative of the overall structural pattern, obviating the need to process the entire dense point cloud. However, the fragment should encompass as wide a range of azimuthal directions as possible.

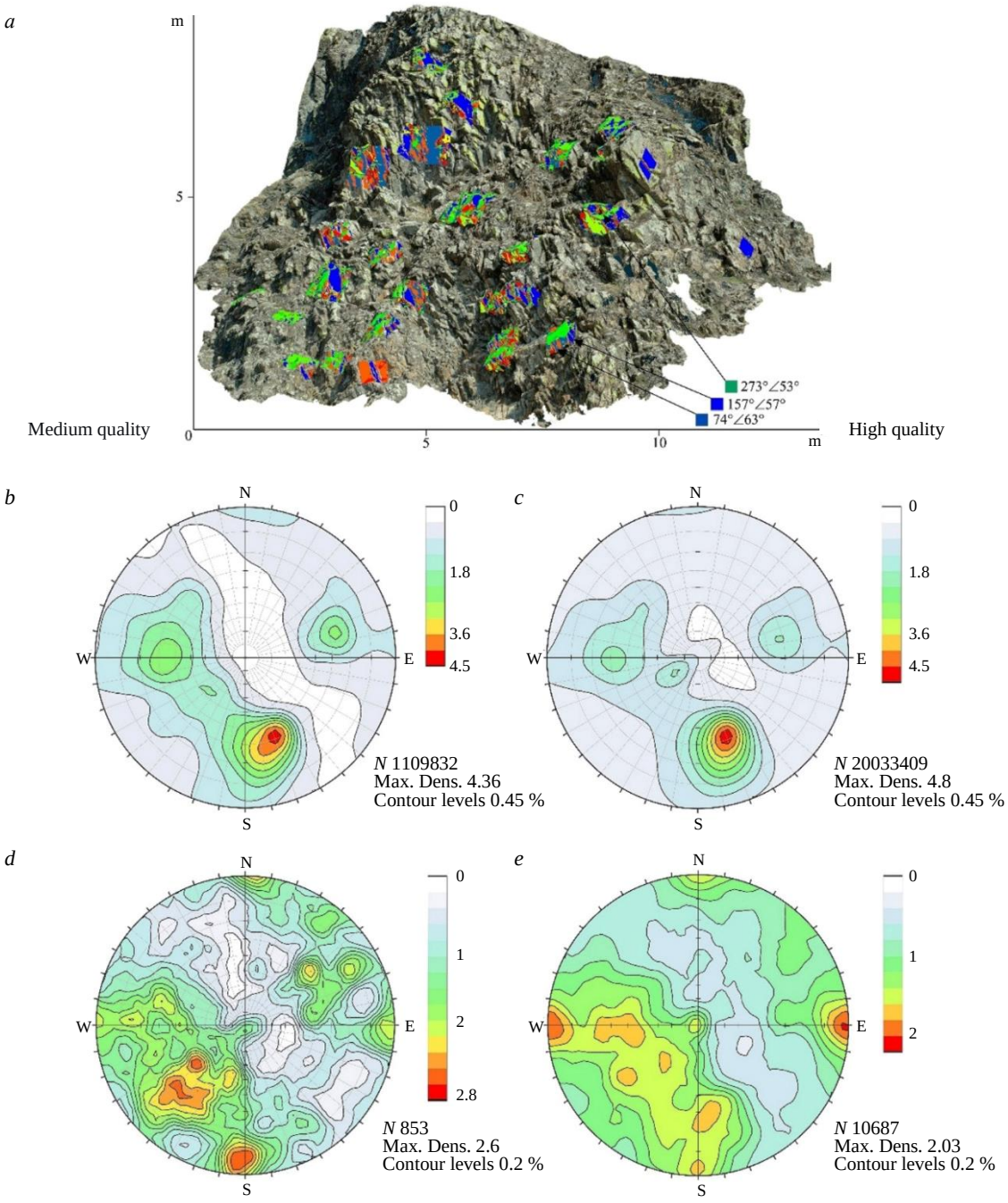


Fig.6. Results of the analysis of dense point clouds from the Sarma outcrop at medium (*b*, *d*) and high (*c*, *e*) resolution:
a – local fragments of the outcrop from which fracture attitudes were extracted and grouped into datasets;
b-e – stereographic projections of poles to fractures extracted using DSE (*b*, *c*) and CloudCompare (*d*, *e*)

This is an open access article under the CC BY 4.0 license

Despite the satisfactory visualization of fracture data in DSE for structural analysis (Fig.5), for solving geomechanical problems, fracture attitudes from DSE are more conveniently visualized in other programs, such as Dips. This is due to the specialized built-in tools for slope stability assessment. However, it should be taken into account that due to the large number of fractures, even with a 1 % contouring window size, Dips performs significant data averaging during construction of the stereoplot, resulting in a reduction in the number of maxima (see Fig.4, *h*) compared to those identified in DSE (see Fig.4, *g*, Fig.5). This issue can be resolved by reducing the number of analyzed fractures through the selection of one or more small fragments of the point cloud model (Fig.6, *a*), following the same approach as used in traditional statistical fracture measurements on a natural outcrop.

A significant challenge in analyzing digital twins is the limited capacity of computers and the time required for data processing. In this regard, an additional experiment was conducted to examine fracture patterns using dense point cloud data of medium and high quality. For this purpose, several small fragments of the digital model of the Sarma outcrop were selected (Fig.6, *a*), from which fractures were extracted and compiled into two datasets. The first dataset consisted of fractures derived from all fragments of the medium-quality dense point cloud, and the second – from the high-quality one. It was found that the stereographic projections of poles to fractures constructed from the DSE data are identical, although the number of fractures in one dataset is 18 times greater than in the other (Fig.6, *b*, *c*). According to the FACETS plugin of CloudCompare, the stereoplots are also generally very similar (Fig.6, *d*, *e*), indicating that for automated fracture extraction and identification of fracture sets, it is sufficient to use a medium-quality dense point cloud generated in Agisoft Metashape.

Conclusion

Modern technical systems and software are evolving rapidly, and their integration into fracture analysis is both inevitable and essential for incorporating the results of structural-geological and tectonophysical studies into the overall technological workflow related to mineral exploration, development, and mining, as well as engineering-geological surveys for the construction of particularly critical facilities. At the same time, their proper application is necessary to obtain reliable results regarding brittle deformations of the Earth's crust, which is facilitated by methodological and experimental studies.

This study has highlighted the main challenges of automated fracture attitude extraction, proposed solutions, and led to the following conclusions:

• The high precision of mathematically extracted fracture dip azimuths and dip angles, combined with their satisfactory correspondence to geological compass-based field measurements, permits the robust use, subject to certain conditions, of the specialized software DSE and the FACETS plugin of CloudCompare for rock fracture analysis. Choosing between these tools because of their distinct algorithms may depend on the outcrop geometry and the size of fracture surfaces oriented toward the camera during data acquisition. Furthermore, when processing large datasets, e.g., exceeding 10,000 extracted fractures, DSE will be a more useful tool for tectonophysical analysis, offering built-in generation of stereographic projections and the ability to resolve a larger number of fracture maxima on them. Along with it, exporting fracture attitude data from both programs to Dips or other software for stereoplot construction will be more appropriate for specific applications.

• An unidirectional survey angle and the exposure of only one wall of the outcrop hinder the identification of diverse fracture sets, since one of them, facing the camera with its dip azimuth, dominates over all others. Although DSE allows determining the main fracture sets with their densities listed in a table, they appear merely as centers of maxima on the stereoplot and are unsuitable for the identification of conjugate fracture sets using some tectonophysical methods (e.g., the Nikolaev method). A multi-directional survey angle and the choice of an outcrop fragment oriented toward different compass directions help avoid unipolarity on the stereographic projections of poles to fractures and enable the acquisition of high-precision data on the structure of the fracture patterns of the rock mass.

This is an open access article under the CC BY 4.0 license

• A properly selected outcrop fragment for calculation reflects its overall structural pattern. This means there is no need to waste time and computer resources analyzing the entire dense cloud. At the same time, if the structural environment changes visually due to a large fault zone, a change in rock type, the need for a detailed study of the quarry walls, or other factors, DOM enable repeated automated analysis of the fracture patterns at any section of the outcrop, including areas that are difficult or even inaccessible to humans, thereby enhancing the quality and productivity of the works.

• Under conditions of limited computing capacity, a dense cloud generated at medium quality in Agisoft Metashape is adequate for extraction of fractures and their associated sets. This approach saves time and computer resources. The high quality of DOM is suitable for visually identification of fractures and other deformation structures.

The potential of using DOM for analyzing the fracture pattern of natural and artificial rock exposures holds great promise for implementation in fundamental research on the Earth's crust structure and in the practice of mining geology. The development of software, including machine learning and neural networks will facilitate this process to identify fractures of various hierarchical levels, calculate their parameters, and construct models of the fault-block environment based on a series of spatially close DOM or on a digital model of an entire quarry. The appropriate use of automated extraction of fracture attitudes and their sets significantly increases the efficiency of studying the deformation characteristics of rocks involved in engineering interventions and mineral deposit development.

REFERENCES

1. Serebryakov E.V., Gladkov A.S. Geological and structural characteristics of deep-level rock mass of the Udachnaya pipe deposit. *Journal of Mining Institute.* 2021. Vol. 250, p. 512-525. DOI: 10.31897/PMI.2021.4.4

2. Chesley J.T., Leier A.L., White S., Torres R. Using unmanned aerial vehicles and structure-from-motion photogrammetry to characterize sedimentary outcrops: An example from the Morrison Formation, Utah, USA. *Sedimentary Geology*. 2017. Vol. 354, p. 1-8. DOI: 10.1016/j.sedgeo.2017.03.013

3. Junjie Zou, Honglin He, Yokoyama Y. et al. A comparative study of bedrock fault scarps by s-UAV and t-LiDAR: Insights into site selection criteria for paleo-seismology studies. *Geomorphology*. 2022. Vol. 414. N 108372. DOI: 10.1016/j.geomorph.2022.108372

4. Koukouvelas I.K., Kyriou A., Nikolakopoulos K.G. et al. Geological and 3D Image Analysis Toward Protecting a Geosite: The Case Study of Falakra, Limnos, Greece. *Minerals*. 2025. Vol. 15. Iss. 2. N 148. DOI: 10.3390/min15020148

5. Na Wu, Zhengzhao Liang, Yan Tao et al. Sensitivity Analysis of Fracture Geometry Parameters on the Mechanical Behavior of Rock Mass with an Embedded Three-Dimensional Fracture Network. *Applied Sciences*. 2022. Vol. 12. Iss. 18. N 9284. DOI: 10.3390/app12189284

6. Tuckey Z. An integrated UAV photogrammetry-discrete element investigation of jointed Triassic sandstone near Sydney, Australia. *Engineering Geology*. 2022. Vol. 297. N 106517. DOI: 10.1016/j.enggeo.2022.106517

7. Birch J.S. Using 3DM Analyst Mine Mapping Suite for Rock Face Characterisation. Laser and Photogrammetric Methods for Rock Face Characterization: Proceedings of the Workshop (Golden, Colorado, June 17-18, 2006. Golden: American Rock Mechanics Association, 2006, p. 13-32.

8. Boos I.Yu., Yunakov Yu.L., Patachakov I.V., Grishin A.A. Structural analysis of pit wall rock mass on 3D slope model constructed using a multicopter. *Mining Informational and Analytical Bulletin*. 2021. N 12, p. 19-30 (in Russian). DOI: 10.25018/0236_1493_2021_12_0_19

9. Riquelme A.J., Abellán A., Tomás R., Jaboyedoff M. A new approach for semi-automatic rock mass joints recognition from 3D point clouds. *Computers & Geosciences*. 2014. Vol. 68, p. 38-52. DOI: 10.1016/j.cageo.2014.03.014

10. García-Luna R., Senent S., Jurado-Piña R., Jimenez R. Structure from Motion photogrammetry to characterize underground rock masses: Experiences from two real tunnels. *Tunnelling and Underground Space Technology*. 2019. Vol. 83, p. 262-273. DOI: 10.1016/j.tust.2018.09.026

11. Monsalve J.J., Pfreundschuh A., Soni A., Ripepi N. Automated Discontinuity Extraction Software Versus Manual Virtual Discontinuity Mapping: Performance Evaluation in Rock Mass Characterization and Rockfall Hazard Identification. *Mining, Metallurgy & Exploration*. 2021. Vol. 38. Iss. 3, p. 1383-1394. DOI: 10.1007/s42461-021-00416-9

12. Dewez T.J.B., Girardeau-Montaut D., Allanic C., Rohmer J. Facets: A CloudCompare plugin to extract geological planes from unstructured 3D point clouds. The International Archives of the Photogrammetry, Remote Sensing and Spatial Information Sciences. ISPRS, 2016. Vol. XLI-B5, p. 799-804. DOI: 10.5194/isprs-archives-XL-B5-799-2016

13. Panara Y., Menegoni N., Carboni F., Inama R. 3D digital outcrop model-based analysis of fracture network along the seismogenic Mt. Vettore Fault System (Central Italy): the importance of inherited fractures. *Journal of Structural Geology*. 2022. Vol. 161. N 104654. DOI: 10.1016/j.jsg.2022.104654

14. Perozzo M., Menegoni N., Crispini L. et al. Quantitative characterization of fracture network in large sheath-fold: field and UAV-based digital outcrop model analysis (Ligurian Alps, Italy). *Journal of Structural Geology*. 2025. Vol. 201. N 105551. DOI: 10.1016/j.jsg.2025.105551

This is an open access article under the CC BY 4.0 license

15. Battulwar R., Emami E., Zare M. et al. Utilizing Deep Learning for the Automated Extraction of Rock Mass Features from Point Clouds. *Geotechnical and Geological Engineering*. 2024. Vol. 42. Iss. 7, p. 6179-6194. DOI: 10.1007/s10706-024-02886-2

16. Buyer A., Schubert W. Calculation the Spacing of Discontinuities from 3D Point Clouds. *Procedia Engineering*. 2017. Vol. 191, p. 270-278. DOI: 10.1016/j.proeng.2017.05.181

17. Riquelme A.J., Tomás R., Abellán A. Characterization of rock slopes through slope mass rating using 3D point clouds. *International Journal of Rock Mechanics and Mining Sciences*. 2016. Vol. 84, p. 165-176. DOI: 10.1016/j.ijrmms.2015.12.008

18. Menegoni N., Giordan D., Inama R., Perotti C. DICE: An open-source MATLAB application for quantification and parametrization of digital outcrop model-based fracture datasets. *Journal of Rock Mechanics and Geotechnical Engineering*. 2023. Vol. 15. Iss. 5, p. 1090-1110. DOI: 10.1016/j.jrmge.2022.09.011

19. Seers T.D., Sheharyar A., Tavani S., Corradetti A. Virtual outcrop geology comes of age: The application of consumer-grade virtual reality hardware and software to digital outcrop data analysis. *Computers & Geosciences*. 2022. Vol. 159. № 105006. DOI: 10.1016/j.cageo.2021.105006

20. Cawood A.J., Bond C.E., Howell J.A. et al. LiDAR, UAV or compass-clinometer? Accuracy, coverage and the effects on structural models. *Journal of Structural Geology*. 2017. Vol. 98, p. 67-82. DOI: 10.1016/j.jsg.2017.04.004

21. Villarreal J. C.A., Rojas D. J.D., Ríos R. C.A. 3D digital outcrop modelling of the Lower Cretaceous Los Santos formation sandstones, Mesa de Los Santos region (Colombia): Implications for structural analysis. *Journal of Structural Geology*. 2020. Vol. 141. N 104214. DOI: 10.1016/j.jsg.2020.104214

22. Triantafyllou A., Watlet A., Le Mouélic S. et al. 3-D digital outcrop model for analysis of brittle deformation and lithological mapping (Lorette cave, Belgium). *Journal of Structural Geology*. 2019. Vol. 120, p. 55-66. DOI: 10.1016/j.jsg.2019.01.001

23. Panara Y., Chandra V., Finkbeiner T. et al. Fracture intensity and associated variability: A new methodology for 3D digital outcrop model analysis of carbonate reservoirs. *Marine and Petroleum Geology*. Vol. 158. Part B. N 106532. DOI: 10.1016/j.marpetgeo.2023.106532

24. Shekov V.A., Ivanov A.A., Krylova S.A. Digital outcrop model as a modern method of geological environment research: the example of Precambrian complexes in Lahdenpohsky district. *Transactions of the Karelian Research Centre of the Russian Academy of Sciences*. 2020. N 10, p. 84-98 (in Russian). DOI: 10.17076/geo1238

25. Nizovtsev A.S., Lunina O.V. Towards new approaches to fracture studies based on UAV aerial photography (examples from Baikal Rift). Continental Rifting, Accompanied Processes: Proceedings of the 5th All-Russian Conference with Participation of Foreign Scientists, Dedicated to the Memory of Academician Nikolay Logatchev on the Occasion of the 95th Anniversary of His Birth, 16-19 April 2024, Irkutsk, Russia. Irkutsk: Izd-vo Irkutskogo gosudarstvennogo universiteta, 2024, p. 96-99 (in Russian).

26. Serebriakov E.V., Gladkov A.S., Gapfarov T.D. Modern methods of data collection for structural damage assessment in rock mass: Review. *Mining Informational and Analytical Bulletin.* 2023. N 9, p. 160-177 (in Russian). DOI: 10.25018/0236_1493_2023_9_0_160

27. Marques Jr. A., Horota R.K., de Souza E.M. et al. Virtual and digital outcrops in the petroleum industry: A systematic review. *Earth-Science Reviews*. 2020. Vol. 208. N 103260. DOI: 10.1016/j.earscirev.2020.103260

28. Battulwar R., Zare-Naghadehi M., Emami E., Sattarvand J. A state-of-the-art review of automated extraction of rock mass discontinuity characteristics using three-dimensional surface models. *Journal of Rock Mechanics and Geotechnical Engineering*. 2021. Vol. 13. Iss. 4, p. 920-936. DOI: 10.1016/j.jrmge.2021.01.008

29. Nurshal M.E.M., Sadewo M.S., Hidayat A. et al. Automatic and Manual Fracture-Lineament Identification on Digital Surface Models as Methods for Collecting Fracture Data on Outcrops: Case Study on Fractured Granite Outcrops, Bangka. *Frontiers in Earth Science*. 2020. Vol. 8. N 560596. DOI: 10.3389/feart.2020.560596

30. Riquelme A., Cano M., Tomás R., Abellán A. Identification of Rock Slope Discontinuity Sets from Laser Scanner and Photogrammetric Point Clouds: A Comparative Analysis. *Procedia Engineering*. 2017. Vol. 191, p. 838-845. DOI: 10.1016/j.proeng.2017.05.251

31. Wen Yan Tung, Nagendran S.K., Ismail M.A.M. 3D rock slope data acquisition by photogrammetry approach and extraction of geological planes using FACET plugin in CloudCompare. *IOP Conference Series: Earth and Environmental Science*. 2018. Vol. 169. № 012051. DOI: 10.1088/1755-1315/169/1/012051

32. Seminsky K.Zh. Specialized mapping of crustal fault zones. Part 1: Basic theoretical concepts and principles. *Geodynamics & Tectonophysics*. 2014. Vol. 5. Iss. 2, p. 445-467 (in Russian). DOI: 10.5800/GT-2014-5-2-0136

33. Sherman S.I., Dneprovskii Yu.I. Stress fields in the Earth's Crust and geological-structural methods of their study. Novosibirsk: Nauka, 1989, p.154 (in Russian).

34. Lunina O.V. The digital map of the Pliocene-Quaternary crustal faults in the southern East Siberia and the adjacent Northern Mongolia. *Geodynamics & Tectonophysics*. 2016. Vol. 7. Iss. 3, p. 407-434 (in Russian). DOI: 10.5800/GT-2016-7-3-0215

35. Makarov S.A. The development history of the Ozerko Valley on the western coast of Lake Baikal. *Geografiya i prirodnye resursy*. 1999. N 4, p. 36-43 (in Russian).

Authors: **Oksana V. Lunina,** *Doctor of Geological and Mineralogical Sciences, Chief Researcher* (*Institute of the Earth's Crust SB RAS, Irkutsk, Russia*), *lounina@crust.irk.ru, https://orcid.org/0000-0001-7743-8877*, **Aleksei S. Nizovtsev,** *Postgraduate Student, Senior Laboratory Assistant* (*Institute of the Earth's Crust SB RAS, Irkutsk, Russia*), *https://orcid.org/0009-0008-1047-0846*.

The authors declare no conflict of interests.

This is an open access article under the CC BY 4.0 license